Polymer 335 (2025) 128816

Contents lists available at ScienceDirect

Polymer

journal homepage: www.elsevier.com/locate/polymer

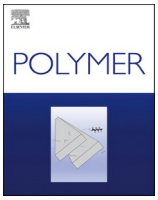

# Mechanochemical and thermal cleavage of polymer linked copper (I)-biscarbene complexes

Philipp Michael [a], Hossam Elgabarty [b], Daniel Sebastiani [b], Wolfgang H. Binder [a,*]

[a] Institute of Chemistry, Chair of Macromolecular Chemistry, Faculty of Natural Sciences II, Martin Luther University Halle-Wittenberg, Von-Danckelmann-Platz 4, 06120, Halle (Saale), Germany
[b] Institute of Chemistry, Chair of Theoretic Chemistry, Faculty of Natural Sciences II, Martin Luther University Halle-Wittenberg, Von-Danckelmann-Platz 4, 06120, Halle (Saale), Germany

ARTICLE INFO

*Keywords:*
Mechanochemistry
Mechanocatalyst
Mechanophore
Click chemistry
Cu-carbene-complexes

ABSTRACT

The force-dependent activation of a latent mechanocatalyst based on polymeric Cu(I)-biscarbene complexes is demonstrated in solution by applied ultrasound, underscoring a mechanochemical activation pathway via an external acoustic field. Systematic experiments via ultrasound mediated activation of the Cu(I)-complex prove a chain length dependent cleavage, favored when longer polymer chains (Mn = 4750; 8900; 17200 g mol$^{-1}$) are attached to the Cu(I)-biscarbene-complex, displaying an subsequent reaction/deactivation pathway with increased ultrasound energy. A different decomposition pathway is observed via purely thermal activation, based on a direct scission of the polymeric chain from the N-heterocyclic carbene, thus prohibiting the formation of the desired catalytically active species. Quantum chemical calculations together with experimental investigations support that splitting one carbene residue from a biscarbene-Cu(I)-center is favored mechanochemically at a force of around 900 pN, in turn lowering the activation energy significantly in comparison to the purely thermal activation pathway.

## 1. Introduction

The cleavage of chemical bonds by mechanical force represents an important tool for triggering chemical reactions, similar to the significantly broader used activation by temperature or photons [1–4]. Mechanochemistry enables access to specific reaction pathways different from their temperature or light-induced counterparts. In polymers, the mechanochemical cleavage of covalent bonds becomes more likely: thus eg. bond rupture either in the solid state [1–3,5–10] is a well known phenomenon applying forces by e.g. compression, ball-milling, tension as well as shear force even in diluted macromolecular solutions [1–3,11] by e.g. external acoustic fields like ultrasound. Therefore, the field of mechanochemistry has become considerably important in macromolecular science [2,4,12], as attached polymer chains allow an more efficient transmission of an applied force to weak links within a macromolecule, in particular addressing bonds of lower energy [1,13].

Covalent bonds in cyclic molecules (such as spiropyranes [6,14], oxiranes [15], *gem*-dihalocyclopropanes [8,16–19], diketenes [20], cyclo-butanes [21–26], or bis-adamantyldioxetanes [27–29]) or in metal complexes (like Ag- and Ru-carbenes [30,31], metal/pincer-complexes [32,33] or metal/multiligand complexes [34–36]) can display a specific mechanochemical activation pathway, often different from their purely thermal or photochemical activation [15–17,20,26]. Thus e.g. in the electrocyclic ring-opening of *cis*-benzocyclobutenes, the disrotatory pathway is favored mechanochemically, whereas the conrotatory pathway proceeds as predicted by the Woodward-Hoffmann rules for the thermally triggered reaction [26].

We here report on the experimental mechanism of mechanochemical as well as thermal cleavage of a polymeric Cu(I)-biscarbene complexes **1** (Fig. 1), onto which polymer chains of different chain length have been attached via *N*-heterocyclic carbene (NHC) linkers. When embedded in linear-polymers [37–39], polymer networks [40,41], peptides [42], or MOFs [43,44], the Cu(I)-biscarbenes can be activated by external mechanical force [4]. Supported by theoretical (CoGEF calculations) and practical investigations, we here do show that a specific mechanochemical pathway prevails, able to split one carbene residue from the biscarbene-Cu(I)-center upon applying external force, in turn lowering

This article is part of a special issue entitled: Bond Breaking in Polymers published in Polymer.

* Corresponding author.
*E-mail address:* wolfgang.binder@chemie.uni-halle.de (W.H. Binder).

https://doi.org/10.1016/j.polymer.2025.128816
Received 10 June 2025; Received in revised form 10 July 2025; Accepted 11 July 2025
Available online 15 July 2025

the activation energy significantly in comparison to the purely thermal activation. The present system is of particular importance, as a subsequent "click"-based chemistry can allow site-specific crosslinking reactions, in turn enabling to activate a "click"-catalyst specifically only at the site of damage and facilitate thus pressure specific self-healing [45–51]. The Cu(I)-biscarbene complexes **1** were designed in compliance with generally accepted requirements for mechanophores. Linear mechanochemical systems including weaker chemical bonds with binding energies of 30–70 kcal/mol [30–36,52] have shown an efficient activation via mechanical force when incorporating the labile bond of a mechanophore in the midst of polymer chains [53–56]. Metal-carbenes in particular reveal the potential to be excellent mechanochemical activation systems, as the metal-carbene bonds are relative stable and chemically inert groups [57,58] but can also be mechanochemically activated by ligand removal, in turn leading to active the metal-catalysts [30,51,59]. An increase in chain length of the used polymers usually favors the transmittance of force onto the middle part of the polymer chains, culminating in bond-cleavage of the most labile bond within the polymer chain [1–3,55,60,61]. Beside the influence of the initial polymer molecular weight, the sonication intensity, the concentration of mechanophores, the temperature as well as the choice of solvent plays an important role on the scission rate of polymers by acoustic fields [19,62–64]. We here report the spectroscopic evidence for specific activation pathways of mechanocatalysts **1**, which proves a mechanochemical activation behavior, in turn generating a catalytically active catalyst.

## 2. Results and discussion

### 2.1. Mechanochemical and thermal decomposition

The mechanophores **1** [51] consist of a centered copper(I) atom linked to two poly (isobutylene) (PIB) chains by *N*-methyl-imidazol-2-ylidene groups, acting as polymeric handles to transmit the applied force to the mechanochemical labile C–Cu bond (see Fig. 1). Three different molecular weights of the polymers were attached ranging from 4750 g $mol^{-1}$ to 17200 g $mol^{-1}$ (Table 1) in order to investigate its influence on the activation behavior. As there is a limitation in the living cationic polymerization with a endgroup fidelity up to about 20 kDa, polymer **1c** is the one with the highest Mn. Additionally, NMR analysis to monitor the subsequent endgroups at higher molecular weights would not be possible due to the endgroup-dilution, then excluding to analyse specific reaction pathways of the Cu-bisNHC segment.

We believe that the attached, highly rigid endgroups (= the Cu-bis NHC) change the adsorption behavior of the polymers during SEC significantly. As the Mn - values determined by NMR are lower than the SEC values and we have used PIB standards to exclude eventual calibration errors from the PS- vs. PIB polymers, we tend to assign this difference to the rigidity of the Cu-bis-NHC middle segment. In addition to NMR-endgroup analysis (see Fig. 4), SEC measurements (Mn, PDIs)

**Table 1**
Investigated Cu(I) mechanocataysts **1** after synthesis via living carbocationic polymerization and subsequent endgroup modification.

| Ent. | Cu(I) catalyst | $M_{n;GPC}$[a] [g $mol^{-1}$] | $M_{n;NMR}$ [g $mol^{-1}$] |
|---|---|---|---|
| **1** | **1a** | 4750 | 2400 |
| **2** | **1b** | 8900 | 5100 |
| **3** | **1c** | 17200 | 8900 |

[a] All values are determined in THF using PIB as standard.

for all polymers during thermal or sonochemical cleavage experiments are provided in Fig. 2A/B. A series of GPC experiments were subsequently conducted to investigate the more detailed influence of ultrasound as well as the thermally induced chain scission of our Cu(I)-mechanophores **1**. Ultrasound is used for activation as it is a generally accepted methodology to simulate stress onto dissolved mechanophores [1,3]. As known from literature [3,13,56,61,62,65–67], a specific mechanochemical activation pathway can be induced by ultrasound in solution by the formation and subsequent collapsing of cavitation bubbles, leading to a defined strain, stretching the polymer molecule until a mechanophore depending scission limit is reached and the most labile bond is cleaved, thus activating the mechanophore. In order to avoid undesired thermal effect during the mechanochemical scission process due to heat generation by collapsing cavitation bubbles, the reactions mixtures were externally thermostated, thus excluding unspecific side reactions [67].

Subjecting the mechanophore samples in THF/MeOH mixtures (concentration 0.75 mM) to ultrasonication revealed a significant decrease of the molecular weight during the sonication process (Fig. 2A). A clear dependency of a symmetric chain cleavage on the sonication time as well as on the initial molecular weight could be observed. With increasing sonication time (represented by different sonication cycles of 90 min ultrasonication with 30 % of max. amplitude of 125 μm and 60 min without sonication) a clear shift to higher retention times and thus smaller molecular weight (with about half of the initial molecular weight 8700 g $mol^{-1}$ when starting from 17200 g $mol^{-1}$) could be observed. This proves the mechanophore fragmentation into smaller fragments via symmetric chain cleavage. Mechanocatalysts with longer polymer chains (**1c**, 17200 g $mol^{-1}$, Fig. 2B) show a significant faster molecular weight degradation compared to those with shorter appended polymer chains (**1a**, 4750 g $mol^{-1}$) proving thus that increased chain length favors the transmittance of force, culminating finally in bond-cleavage of the most labile bond close to the midst point of the polymer chain [1–3,55,60,61].

In order to compare the individual cleavage efficiencies, a (semi-) quantification of the GPC traces was accomplished by calibrating the RI-signal intensity to the concentration of the polymeric bis- (**1**) and monocarbene (**2**) moieties (for details see Supporting Information). Results are summarized in Table 2 and depicted graphically in Fig. 2C. The highest content (~84 %) of cleaved mechanophore by ultrasound was observed for the longest catalyst **1c** (Mn = 17200 g $mol^{-1}$), while in

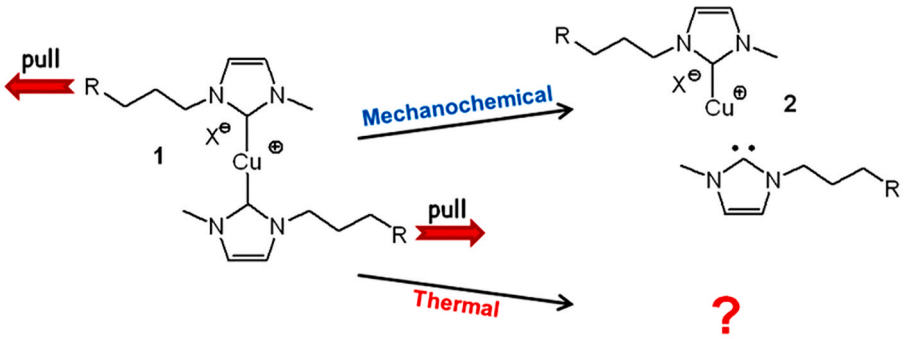


**Fig. 1.** Mechanochemical versus thermal activation of polymeric Cu(I)-biscarbene mechanocatalyst **1** (R = propoxyphenyl telechelic polyisobutylene (PIB)).

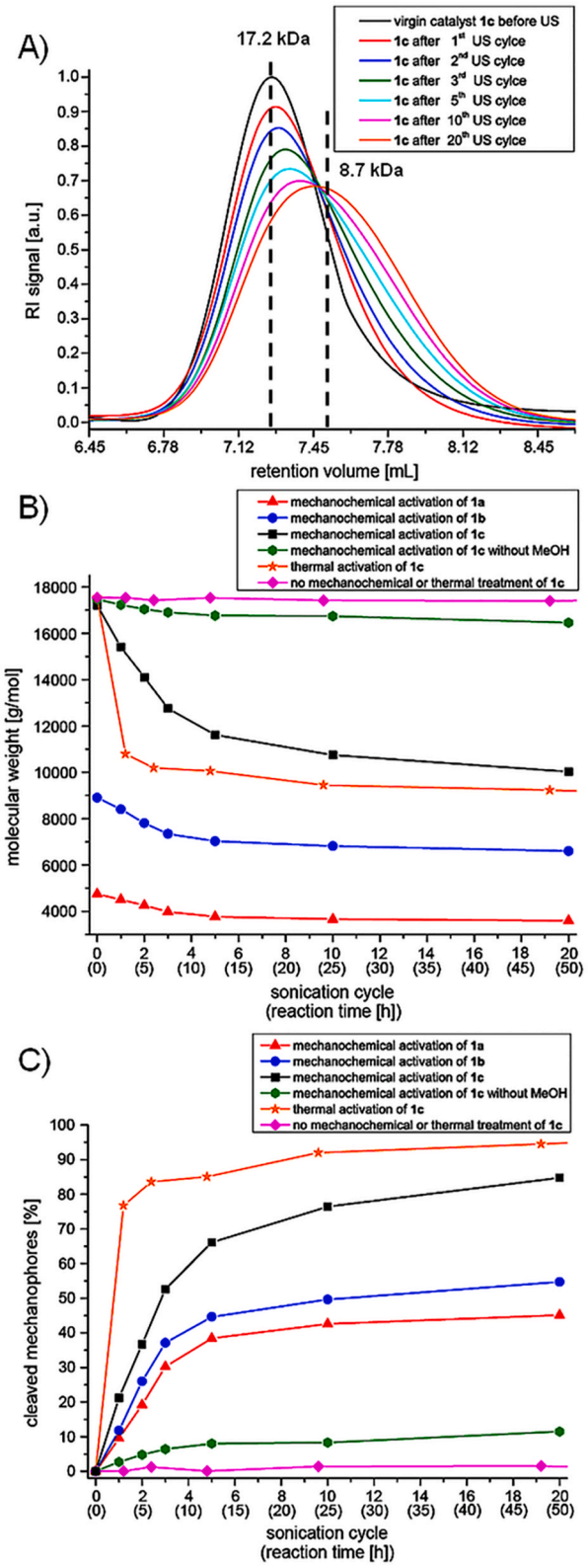


**Fig. 2.** (A) GPC traces of the virgin catalyst **1c** before ultrasonication (black) and decreasing molecular weight indicated by increased retention volume after multiple sonication cycles. (B) Decreasing molecular weight of **1** (determined by GPC) versus the sonication time depending on the initial molecular weight and sonication conditions. (C) Cleavage of mechanocatalyst **1** depending on the initial molecular weight and sonication conditions.

**Table 2**
Cleavage of mechanocatalysts **1a-c** with different molecular weights under different cleavage conditions (for time dependent values see Supporting information).

| Ent | $Cu^{I}$ cat | US cycles[a] | T [°C] | solvent | PDI | | cleaved mechano-phores[b] [%] |
|---|---|---|---|---|---|---|---|
| | | | | | initial | end | |
| ***1*** | ***1a*** | *20* | *20* | *THF/ MeOH* | *1.6* | *1.8* | *45* |
| ***2*** | ***1b*** | *20* | *20* | *THF/ MeOH* | *1.2* | *1.5* | *55* |
| ***3*** | ***1c*** | *20* | *20* | *THF/ MeOH* | *1.2* | *1.5* | *84* |
| ***4*** | ***1c*** | *20* | *20* | *THF* | *1.2* | *1.2* | *11* |
| ***5*** | ***1c*** | - | *65* | *THF/ MeOH* | *1.2* | *1.5* | *97* |
| ***6*** | ***1c*** | - | *20* | *THF/ MeOH* | *1.2* | *1.2* | *0* |

[a] Ultrasonicaton cycle: 90 min sonication with 30 % of max. amplitude of 125 μm with pulse sequence 5s on, 10s off and 60 min without sonication.
[b] Determined after 20 sonication cycles (50h) for entries 1–4 and after 72h for entries 5–6 from GPC values according to equation Seq 1 (see supporting material).

case of the shortest mechanocatalysts **1a** (Mn = 4750 g $mol^{-1}$) only ~ 45 % of the chains were cleaved after the same sonication time. An almost linear decrease of the molecular weight and thus a linear increase of mechanochemical cleaved catalysts could be observed for the first three sonication cycles up to 7.5 h independently on the initial molecular weight (Fig. 2B and C). After 5 cycles of sonication, the curve converges slowly to the aforementioned final values, indicating a significantly slower cleavage of the smalls chains by ultrasound [68]. Additionally, a broadening of the molecular weight distribution (PDI) e. g. from 1.2 to 1.5 for **1c** could be observed (Table 2).

The effect of the methanol addition was investigated as MeOH is able to protonate the cleaved carbenes in turn preventing the back reaction with the Cu(I)-monocarbene complex **2** (Fig. 3). Using pure tetrahydrofuran (THF) without MeOH leads to a significantly lower activation of the mechanophores, e.g. 11 % for **1c** compared to 84 % when THF/MeOH 30:1 mixtures were used (Fig. 2, Table 2 entries 3 + 4). Control experiments were conducted by monitoring the molecular weights of **1** by GPC without ultrasound or thermal treatment. In all cases no significant chain scission could be observed (Fig. 2B and C, Table 2 entry 6). Furthermore, the pure thermal activation behavior of the mechanophores **1** was investigated by GPC. Subjecting **1** to a purely thermal treatment (65 °C for 72 h) also leads to chain scission (Fig. 2, Table 2 entry 5), although the resulting catalyst does not show catalytic activity (vide supra).

To elucidate the chemical species after mechanochemical or thermal cleavage, both, the mechanochemical and thermal reactions were investigated in more detail by *in-situ* $^{1}$H NMR spectroscopy. Therefore, the mechanocatalysts **1** were subjected to either to mechanochemical force by ultrasonication or thermal treatment (at 65 °C). Fig. 4A shows the $^{1}$H NMR spectra for the mechanochemical cleavage of **1c** as virgin catalyst and after the 1st, 2nd, 3rd, 5th, 10th and 20th sonication cycle. Indeed we observe a change in mechanism after the 3rd sonication cycle. Although the amounts of the activated/decomposed catalyst are truly small, we however see in the first two cycles a clear (expected) carbene removal, which then moves into the destructive (and obviously nonreversible pathway) as described in Fig. 4. Before ultrasonication only the resonances of the virgin catalyst **1** (NC*H*–C*H*N at 6.25 and 6.20 ppm, phenoxy group at 6.81 ppm) were visible. Ultrasonication up-to the 3rd sonication cycle led to an increasing amount of the cleaved monocarbene species **2** (visible at 6.40 and 6.63 ppm NC*H*–C*H*N, phenoxy group at 6.75 ppm) as well as of the protonated macroligand **3** (NC*H*N at 9.98 ppm, phenoxy group at 6.85 ppm), proving the specific cleavage of the Cu-carbene-bond in the mechanophore **1** (Fig. 3) together with

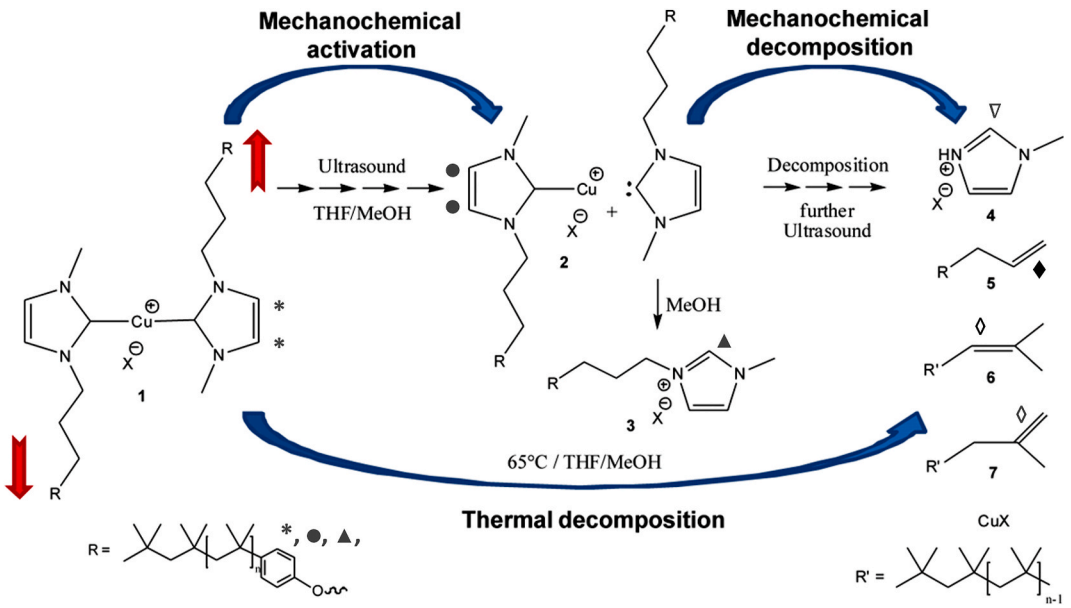


**Fig. 3.** A) Mechanochemical activation of polymeric biscarbene Cu(I) complex (**1**) by ultrasound forming the catalytic active monocarbene complex (**2**) and further decomposition to degradation products **4**–**7**. B) Thermal decomposition of **1** (T = 65 °C) without intermediate activation. (Labeled protons of mechanocatalyst and its degradation products (* - 1; ● - 2; ▲ - 3; ▽ - 4; ◆ - 5; ◊ - 6 + 7), corresponding to the NMR peaks presented in Fig. 4).

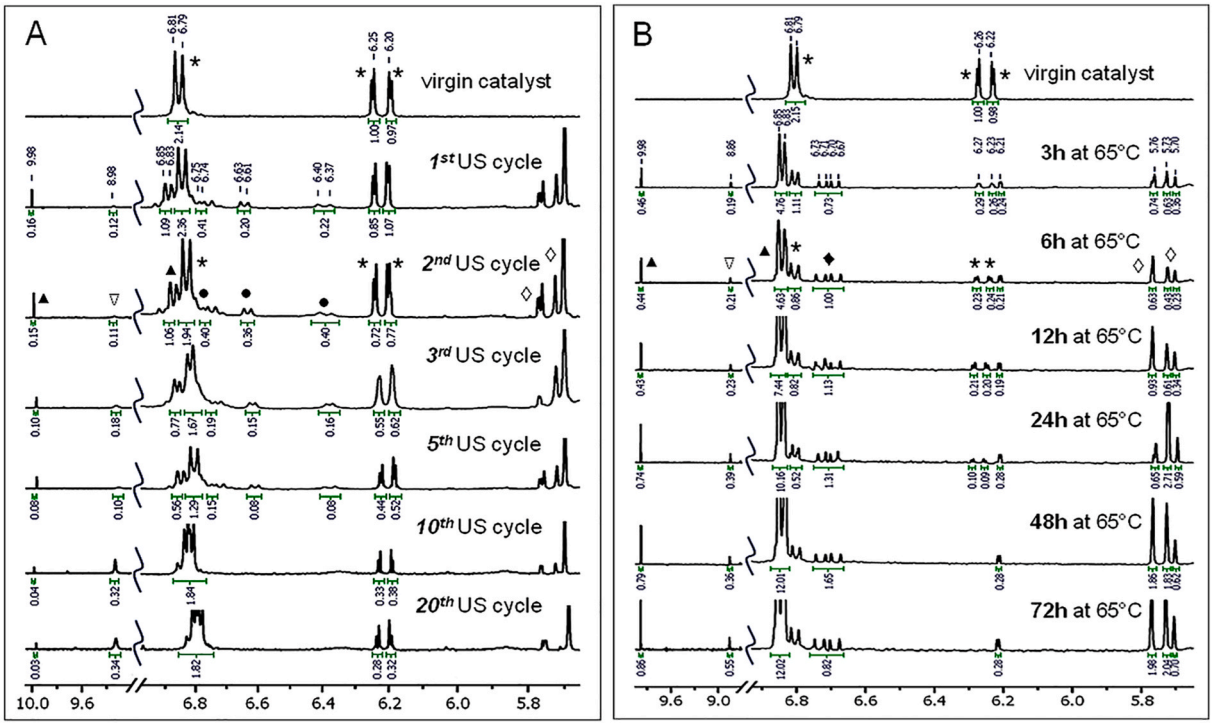


**Fig. 4.** $^{1}$H NMR spectroscopic investigations of activation and decomposition of [Cu(PIB-NHC)$_2$]X catalyst (**1c**). (A) Mechanochemical cleavage of **1c** using ultrasound in multiple cycles of 90 min sonication and 60 min intermission indicating the formation of catalytic active monocarbene species **2c** and their subsequent decomposition to degradation products **4**–**7**. (B) Time dependent thermal decomposition of **1c** at 65 °C without intermediate activation generating directly the degradation products **4**–**7**. (* - **1**; ● - **2**; ▲ - **3**; ▽ - **4**; ◆ - **5**; ◊ - **6** + **7** – highlighted in Fig. 3).

another reaction pathway.

Thus after the 3rd sonication cycle the intensity of the monocarbene species **2** decreases until its complete disappearance after the 10th cycle (Fig. 4A) revealing the further decomposition of the Cu(I)-monocarbene complex **2** with ultrasonication. The additional resonances (at 8.98 ppm and around 5.75 ppm) can be assigned to the decomposition products **4**–**7**, formed by either the elimination of the methylimidazol-2-ylidene end group or the complete elimination of the methylimidazol-2-ylidene bearing phenoxy end group from the PIB chain generating internal and terminal double bonds (see Fig. 3). These observations proved a change in the decomposition pathway of **1** after the third sonication cycle form the desired ultrasound induced cleavage into **2** and **3** to a destructive mechanism leading to a breakdown of the polymer-carbene scaffold.

Similar the purely thermal activation behavior of the mechanophores **1** was investigated. Fig. 4B shows the $^1$H NMR spectra of the thermally treated mechanophore **1c** after 3, 6, 12, 24, 48 and 72 h, indicating strong changes after 3 h heating at 65 °C in compliance to the observed chain scission observed by the GPC investigations. No formation of the Cu(I)-monocarbene species **2** could not be observed, instead the formation of the re-protonated *N*-methylimidazol-2-ylidene telechelic PIB macroligand **3** (9.98 ppm) as well as the elimination products **4**–**7** (8.86, 5.76, 5.73 and 5.70 ppm) were seen, clearly proving a different decomposition of the catalyst **1** via the thermal pathway, further supporting the obtained GPC results. In contrast to the mechanochemical pathway (Fig. 3), no formation of the catalytic active Cu(I)-monocarbene species **2** could be observed, resulting in the direct formation of the elimination products **4**–**7**.

In both cases - the sonication-induced as well as the thermally-triggered scission - the formation of solid particles could be monitored and flame atomic absorption spectroscopy (FAAS) proved the presence of copper in significant amounts within the particles. Probing the exact nature of the copper species via STEM-EDXS measurements revealed the presence of Cu and O in a ratio of 63.4 : 36.6 (≈2 : 1), indicating the formation of copper(I)-oxide ($Cu_2O$) (Fig. 5). The small, brighter region on the left side of the particle consist predominantly out of $Cu_2O$ but contains also Cu(II) halides (Br, I). The formation of these copper nanoparticles supports the decomposition of the Cu(I)-monocarbene complex **2** by ultrasound in the presence of oxygen traces. Blind experiments in the absence of ultrasonication or thermal treatment were performed without significant changes in $^1$H NMR or the formation of particles even after one week.

### 2.2. Catalytic activity in a mechanochemical "click" reaction

In order to prove the catalytic activity of the cleaved mechanocatalysts **1** after activation by ultrasound or thermal activation, a model copper(I)-catalyzed alkyne/azide "click" reaction (CuAAC) of benzyl azide (**8**) with phenylacetylene (**9**) was performed (Table 3).

Mechanophores **1a-c** were subjected to several ultrasonication cycles and the conversion of "click" reaction was monitored by *in-situ* $^1$H NMR spectroscopy after the 1st, 2nd, 3rd, 5th and 10th cycle and compared to the conversions observed via thermal activation. Initially, the latent catalysts **1** display no catalytic activity in their inactive origin state irrespective of their initial molecular weight when not subjected to either ultrasonication or thermal treatment (**1c**, Table 3 entry 5, Fig. 6). As the application of ultrasound to the mechanocatalysts **1** leads to a cleavage of one of the shielding polymeric-NHC ligands an activation of the latent catalysts under formation of an active Cu(I)-monocarbene complex **2** is expected. The observed catalytic activity scaled directly with the initial chain-length of the attached polymer chains: increasing Mn from 4750 g mol$^{-1}$ (**1a**) to 17200 g mol$^{-1}$ (**1c**) lead to a "click"

**Table 3**
Time and sonication cycle dependent investigation of click reaction from benzyl azide (**8**) and phenylacetylene (**9**) using [Cu(PIB-NHC)$_2$]X catalysts (**1**).[a]

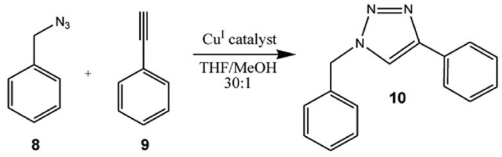


| Ent | Cu(I) catalyst | T [°C] | US[b] | Conversion after US cycle[c] [%] | | | | | |
|---|---|---|---|---|---|---|---|---|---|
| **A** | **Mechanochemical** | | cylce | 0 | 1 | 2 | 3 | 5 | 10 |
| | | | t [h] | 0 | 2.5 | 5 | 7.5 | 12.5 | 25 |
| **1** | without | 20 | on | 0 | 0 | 0 | 0 | 0 | 0 |
| **2** | **1a** | 20 | on | 0 | 2 | 8 | 10 | 10 | 11 |
| **3** | **1b** | 20 | on | 0 | 6 | 14 | 16 | 18 | 19 |
| **4** | **1c** | 20 | on | 0 | 6 | 17 | 26 | 28 | 28 |
| **5** | **1c** | 20 | off | 0 | 0 | – | 0 | – | 0 |
| **B** | **Thermal** | | t [h] | 0 | 3 | 6 | 12 | 24 | 72 |
| **6** | **1c** | 65 | off | 0 | 0 | 0 | 0 | 1 | 3 |

[a] For all reaction an equimolar mixture of **8** and **9** in THF/MeOH 30:1 where used together with 0.01 equiv. of mechanocatalyst **1** (c = 0.75 mM).
[b] Each ultrasonication cycle consists of 90 min sonication with 30 % of max. amplitude of 125 μm with pulse sequence of 5 s on, 10 s off and 60 min without sonication.
[c] Determined by $^1$H NMR spectroscopy in THF-$d_8$/MeOH 30:1 monitoring the increasing triazole resonance at $\delta$ = 8.12 ppm as well as the shift of the $CH_2$ resonance from $\delta$ = 4.34–5.58 ppm.

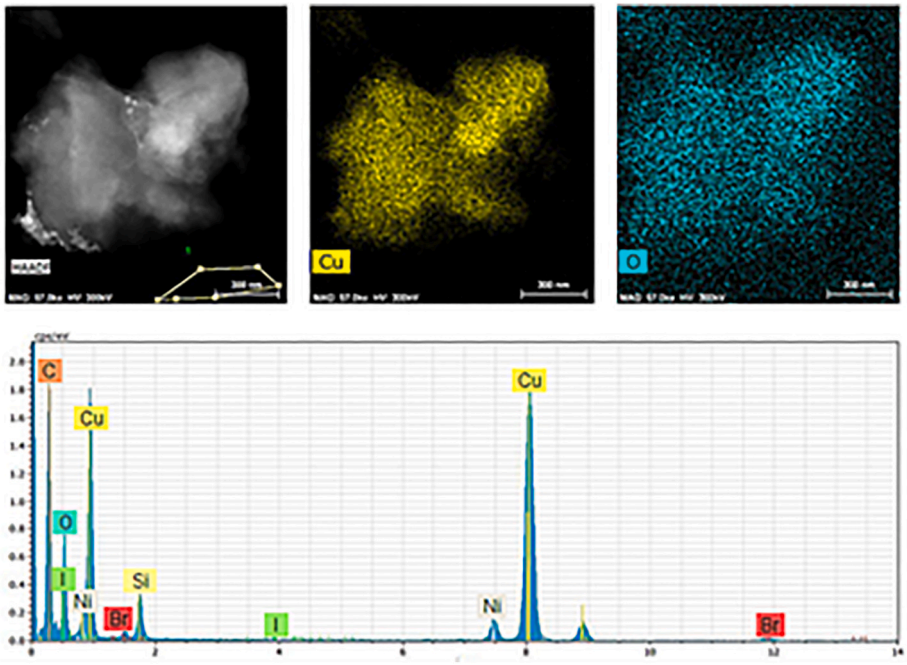


**Fig. 5.** STEM-EDXS of Cu-precipitates obtained during cleavage of mechanophores **1**.

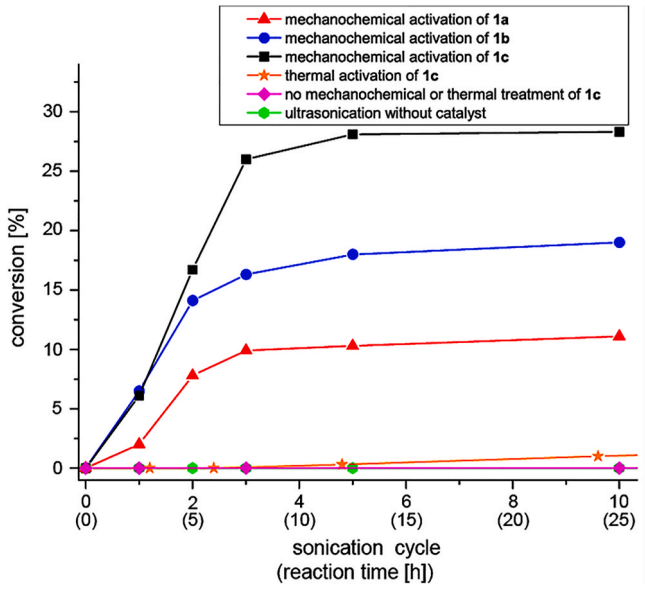


**Fig. 6.** Time and sonication cycle dependent investigation of click reaction from an equimolar mixture of benzyl azide (**8**) and phenylacetylene (**9**) in THF/MeOH 30:1 (75 mM) using $[Cu(PIB\text{-}NHC)_2]X$ (**1**) catalysts (0.75 mM) under sonication of pure thermal activation (for more detailed information see supporting information).

conversion from 11 to 28 % after 10 sonication cycles (Table 3 entries 2–4). Analyzing the time dependent $^1$H NMR measurements reveal a saturation of the "click" conversion after the third sonication cycle, irrespective of the initial molecular weight of the mechanophore (Fig. 6), in compliance with the observations of GPC as well as the $^1$H NMR investigations described before, where the amount of the monocarbene-species **2** also reaches saturation after the third cycle.

Thermally induced scission of the mechanocatalysts **1** by heating to 65 °C induces only a poor reactivity below 3 % conversion in the CuAAC reaction of **8** and **9** (Table 3 entry 6, Fig. 6) indicating no or neglectable amount of catalytic active monocarbene species **2**. The reduction of the molecular weight observed in the pure thermal scission of **1** in GPC experiments thus does not lead to catalytically active Cu-carbene species, as also discussed via 1-NMR-spectroscopy (see Fig. 3).

### 2.3. Theoretical modeling of mechanochemical activation

In order to corroborate our practical observations, we performed a series of constrained geometry optimizations under the influence of an external pulling force [26,60,61,69,70] employing the CoGEF method (Constrained Geometries simulate External Force [60]). In recent years, such theoretical models have been successfully used to investigate and rationalize the response of covalent bonds to external mechanical forces, whether in the context of a single molecule in atomic force microscopy or in ultrasonication experiments. Forces computed using CoGEF are typically a bit larger than the true experimental forces. In this method a static geometry is considered (for all degrees of freedom except the constrained reaction coordinate), while in nature, all degrees of freedom are subject to vibrations, which are coupling to the reaction coordinate and have the potential to lower the force at which the bond cleavage occurs. In our work, the application of the CoGEF calculations is to determine the influence of an additional external force (applied to the molecular extremities) to the remaining force that is required for achieving a given bond rupture. In this setting, all the vibrational effects (that the CoGEF scheme ignores) apply to all computed conformations in the same way, so that the error largely cancels. The true rupture forces are certainly shifted with respect to more realistic calculations, but the mechanochemical effect of the additional force is most probably well reproduced.

The most simple theoretical models for breaking covalent bonds by mechanical force are one-dimensional models based on the Bell model [71] and its extensions (e.g. the "tilted potential energy surface model" [72,73] and the "extended Bell model" [74]). These models essentially require knowledge of the activation energy at zero force employing subsequently a truncated Taylor expansion of a force-dependent one-dimensional potential energy surface to estimate the activation energy under a given force. Going beyond one-dimensional models is especially important if the focus of interest is on structure reactivity parameters or whenever catch-bonds or anti-Hammond effects are important [75,76].

To investigate the force-dependence of the dissociation barrier, constrained geometry optimization calculations in the presence of external mechanical forces were employed. Starting from the geometry optimized structure of **1** (with R═H), a series of constrained geometry optimizations were performed at different external forces (0 pN–900 pN

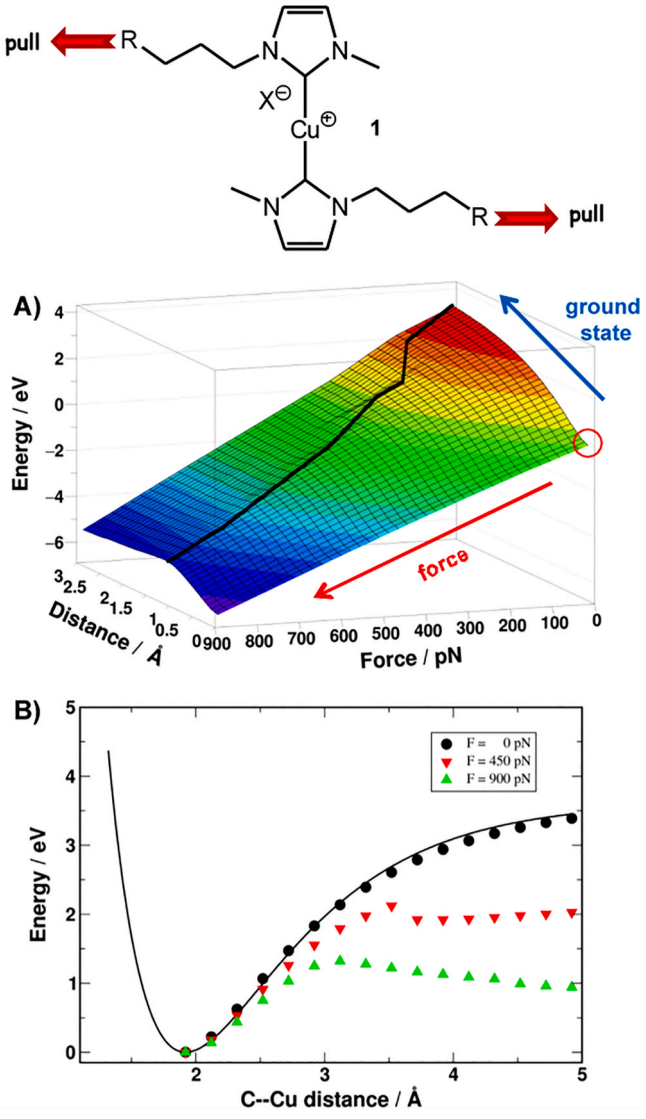


**Fig. 7.** CoGEF calculations for geometry optimized structure of mechanocatalyst **1** (with R═H). A) The force-tilted potential energy surface of C–Cu bond cleavage. The energies and distances are references to the optimized geometry in the absence of external force, marked by the red circle. The bold line traces the position of the maximum as a function of the pulling force. B) Pulling force-dependence of one-dimensional energy profiles. All the curves are shifted to 0 eV at the first point. (For interpretation of the references to colour in this figure legend, the reader is referred to the Web version of this article.)

in steps of 150 pN), where the force was always applied to the terminal carbon of the alkyl chain, along the direction shown in Fig. 7.

The results of the CoGEF scan are depicted in Fig. 7A, wherein both trends characteristic for covalent mechano-cleavage can be seen. With increasing external force, the potential energy barrier drops down to 1.2 eV at a force of 900 pN. The force required for mechanical scission is one order of magnitude less than the typical values for covalent C–C bond cleavage and falls within the expected range for an organometallic bond [61]. Similarly, the C–Cu distance of the transition state (traced along the top of the hill running diagonally down the plot), moves closer to the equilibrium geometry at a force of 0 pN, i.e. the Hammond effect. One-dimensional plots are depicted in Fig. 6B for selected values of the external pulling force. The maximum slope of these one-dimensional energy profiles corresponds to the maximum force required to break the bond. The external force-dependence of the maximum slope shows an almost perfect linear trend with a slope of −0.1, indicating the maximum force required to break the bond is decreased by exactly the value of the external pulling force (see Supporting Information). The computational results indeed support the experimental data (also supported by SFMS-experiments [37]) indicating that external mechanical force is able to induce the cleavage of one C–Cu bond generating a free catalytic site. This bond is the weakest point in the dimerized polymer chains and is thus expected to be the preferred point of cleavage under applied external force via ultrasonication.

## 3. Conclusions

In summary, experimental and quantum chemical calculations (CoGEF) investigations prove that a polymer based Cu(I)-biscarbene catalyst **1** can be activated via two different pathways: a mechanochemical reaction pathway (induced by ultrasound) under formation of a catalytic active Cu(I)-monocarbene complex **2** via specific cleavage of the Cu–N bond of the NHC-carbene, and a thermal pathway, leading to chain scission of the N–C bond of the attached polymer chain, and thus the absence of the specific carbene-cleavage. At longer ultrasonication times a further decomposition of the catalytic active species **2** is caused leading to $Cu_2O$/Cu(II)-halide-species, similar to the thermal activation. Mechanochemical scission up to ~84 % of the mechanophores could be observed, increasing with increasing molecular weight of the attached polymers. In contrast, thermal treatment caused a direct decomposition of the mechanocatalyst without intermediate activation displaying no significant catalytic activity of **1** towards the "click" reaction. The obtained results are unique as now distinctly different reaction pathways can be controlled for a Cu-carbene-catalyst. Such mechanocatalysts are highly attractive systems for transforming stress into chemical reactions [37 - 44] via specific catalytic systems - for e.g. stress reporting as well as self-healing in polymeric materials.

## 4. Experimental

### 4.1. Materials and methods

All chemicals were purchased from Sigma-Aldrich and used without further purification unless noted. All NMR spectra were recorded on a Varian Gemini 400 spectrometer at 400 MHz at 27 °C in $CDCl_3$ (Armar Chemicals, 99.8 Atom%D) or THF-$d_8$ (Armar Chemicals, 99.8 Atom%D) respectively. Gel permeation chromatography (GPC) was performed on a Viscotek GPCmax VE 2002 using a column set of CLM3008 and GMHHR-N-18055 in THF (VWR Prolabo, HPLC grade) with a column temperature of 22 °C, an injection volume of 100 μL and a flow rate of 1 mL/min. Detection was accomplished by refractive index on a VE 3580 RI detector of Viscotek at 35 °C. External calibration was done using PIB standards (purchased form Polymer Standards Service in a molecular weight range from 340 to 87600 g $mol^{-1}$). All experiments were repeated at least twice and display the same results with maximum deviation of ±2 %. STEM-EDXS analyses (*S*canning *T*ransmission *E*lectron *M*icroscopy - *E*nergy *D*ispersive *X*-ray *S*pectroscopy) were performed on FEI TITAN$^3$ G2 80–300 using carbon-coated Ni TEM grids. The sample preparation was done by ultrasonic dispersion of the powder in isopropyl alcohol, followed by putting one droplet of the dispersion onto the TEM grid and drying on a hot plate. Poly (isobutylene) (PIB) based mechanocatalysts (**1**) were synthesized according to previously published procedure [51].

### 4.2. Sonication experiments

Ultrasonication experiments were performed with a Sonics VCX 500 ultrasonic processor at a frequency of 20 kHz. A 254 mm long full wave solid probe out of titanium alloy (Ti–Al–4V) with a diameter of 13 mm was used together with an internally threaded stainless steel adapter (fitting to probe at nodal point). All sonication experiments were conducted under inert and dry conditions in a 10 mL reaction vessel with two additional 14/20 side necks which was temperate at 20 °C by an external cooling bath. The mixtures of mechanocatalysts **1** were prepared either in pure THF or in 30:1 THF/MeOH mixtures according to common Schlenk techniques. In case of NMR investigations deuterated THF as well as non deuterated MeOH were used as solvents, while HPLC grade solvents were used for GPC experiments. The mechanophore concentration was adjusted in compliance to literature [31,68] to 0.75 mM. Subsequently, ultrasound was applied with 30 % of the maximal amplitude of 125 μm in several sonication cycles. One cycle consists of 90 min sonication (with a pulse sequence of 5s on and 10s off) followed by 60 min without sonication. NMR as well as GPC samples were directly taken out of the mixture at the end of the 1st cycle after 150 min, 2nd cycle after 300 min, 3rd cycle after 450 min, 5th cycle after 750 min, 10th cycle after 1500 min and 20th cycle after 3000 min.

### 4.3. Thermal experiments

Thermal decomposition experiments were conducted under dry and inert conditions in normal two-necked flasks without ultrasonication. The mechanophore concentration was kept constant at 0.75 mM, while the temperature was adjusted to 65 °C under reflux conditions in THF/MeOH 30:1. NMR or GPC samples were directly taken out of the mixture after appropriate time. Blind experiments were conducted applying the same conditions at room temperature.

### 4.4. Investigation of catalytic activity

The catalytic activity of mechanocatalysts **1** was investigated by means of a model "click" reaction from benzyl azide (**8**) and phenylacetylene (**9**). For that purpose, an appropriate amount of **1** was weight directly into the reaction vessel for ultrasound application (see above) and subjected to several vacuum-argon cycles. Subsequently, an equimolar mixture of **8** and **9** (100 equivalents per catalyst each) were prepared in THF-d8/MeOH 30:1 in a concentration of 75 mM under dry and inert conditions and were transferred to the reaction vessel. Ultrasound was applied in several sonication cycles using the same setup described above. Thermal experiments were performed under inert conditions in normal two-necked flasks equipped with condenser. The concentrations kept the same as for sonication experiments. In both cases, the NMR samples were taken directly out of the mixture at appropriate times.

### 4.5. Theoretical calculations

To investigate the force-dependence of the dissociation barrier, constrained geometry optimization (CoGEF) calculations in the presence of external mechanical forces were employed. Starting from the geometry optimized structure (Figure 7, **1** with R═H), a series of constrained geometry optimizations were performed at different external forces (0 pN–900 pN in steps of 150 pN), where the force was always applied to

the terminal carbon of the alkyl chain, along the direction shows in Fig. 7. For each chosen value of external force, one of the carbene carbons distances to copper was constrained at a particular value, which was scanned in steps of 0.2 Å.

All calculations were preformed with the CP2K [77] code using the GGA PBE exchange-correlationfunctional [78] plus a damped interatomic potential to account for van der Waals interactions [79], a plane wave density cutoff of 500 Ry, with Goedecker–Teter–Hutter pseudopotentials and an accurate triple-zeta atom-centered Gaussian basis set with two sets of polarization functions (TZV2P) [80]. In order to perform calculations on an isolated cluster, a wavelet Poisson solver was employed to decouple the periodic potential [81].

## CRediT authorship contribution statement

**Philipp Michael:** Writing – original draft, Investigation, Formal analysis, Data curation, Conceptualization. **Hossam Elgabarty:** Writing – review & editing, Methodology, Formal analysis, Data curation, Conceptualization. **Daniel Sebastiani:** Writing – original draft, Validation, Supervision, Formal analysis. **Wolfgang H. Binder:** Writing – original draft, Validation, Supervision, Funding acquisition, Formal analysis, Conceptualization.

## Declaration of competing interest

The authors declare the following financial interests/personal relationships which may be considered as potential competing interests: Prof. Dr. Wolfgang H. Binder reports a relationship with Martin Luther University Halle Wittenberg that includes: employment and funding grants. If there are other authors, they declare that they have no known competing financial interests or personal relationships that could have appeared to influence the work reported in this paper.

## Acknowledgements

This work was financed by the PoliFaces Initiative/State of Saxony-Anhalt, EM3.

“Preparatory Cluster within the framework of the Federal Excellence Strategy: Polymer Sustainability”. This research was supported by the German Science Foundation, DFG-projects BI 1337/17–1, BI1337/18–1, and European Regional Development Fund (EFRE).

## Appendix A. Supplementary data

Supplementary data to this article can be found online at https://doi.org/10.1016/j.polymer.2025.128816.

## Data availability

Data will be made available on request.

## References

[1] M.K. Beyer, H. Clausen-Schaumann, Mechanochemistry: the mechanical activation of covalent bonds, Chem. Rev. 105 (8) (2005) 2921–2948, https://doi.org/10.1021/cr030697h.
[2] P.A. May, J.S. Moore, Polymer mechanochemistry: techniques to generate molecular force via elongational flows, Chem. Soc. Rev. 42 (18) (2013) 7497–7506, https://doi.org/10.1039/c2cs35463b.
[3] M.M. Caruso, D.A. Davis, Q. Shen, S.A. Odom, N.R. Sottos, S.R. White, J.S. Moore, Mechanically-induced chemical changes in polymeric materials, Chem. Rev. 109 (11) (2009) 5755–5798, https://doi.org/10.1021/cr9001353.
[4] W.H. Binder, The “labile” chemical bond: a perspective on mechanochemistry in polymers, Polymer 202 (2020) 122639, https://doi.org/10.1016/j.polymer.2020.122639.
[5] Y. Chen, A.J. Spiering, S. Karthikeyan, G.W. Peters, E.W. Meijer, R.P. Sijbesma, Mechanically induced chemiluminescence from polymers incorporating a 1,2-dioxetane unit in the main chain, Nat. Chem. 4 (7) (2012) 559–562, https://doi.org/10.1038/nchem.1358.
[6] D.A. Davis, A. Hamilton, J. Yang, L.D. Cremar, D. Van Gough, S.L. Potisek, M. T. Ong, P.V. Braun, T.J. Martinez, S.R. White, J.S. Moore, N.R. Sottos, Force-induced activation of covalent bonds in mechanoresponsive polymeric materials, Nature 459 (7243) (2009) 68–72, https://doi.org/10.1038/nature07970.
[7] R.T.M. Jakobs, S. Ma, R.P. Sijbesma, Mechanocatalytic polymerization and cross-linking in a polymeric matrix, ACS Macro Lett. 2 (7) (2013) 613–616, https://doi.org/10.1021/mz400201c.
[8] J.M. Lenhardt, A.L. Black, B.A. Beiermann, B.D. Steinberg, F. Rahman, T. Samborski, J. Elsakr, J.S. Moore, N.R. Sottos, S.L. Craig, Characterizing the mechanochemically active domains in -dihalocyclopropanated polybutadiene under compression and tension, J. Mater. Chem. 21 (23) (2011) 8454–8459, https://doi.org/10.1039/c0jm04117c.
[9] L. Rinaldi, K. Martina, F. Baricco, L. Rotolo, G. Cravotto, Solvent-free copper-catalyzed azide-alkyne cycloaddition under mechanochemical activation, Molecules 20 (2) (2015) 2837–2849, https://doi.org/10.3390/molecules20022837.
[10] C. Xu, S. De, A.M. Balu, M. Ojeda, R. Luque, Mechanochemical synthesis of advanced nanomaterials for catalytic applications, Chem. Commun. 51 (31) (2015) 6698–6713, https://doi.org/10.1039/c4cc09876e.
[11] C.L. Brown, S.L. Craig, Molecular engineering of mechanophore activity for stress-responsive polymeric materials, Chem. Sci. 6 (4) (2015) 2158–2165, https://doi.org/10.1039/c4sc01945h.
[12] R. Boulatov, Polymer mechanochemistry. Topics in Current Chemistry, Springer International Publishing, Heidelberg, 2015.
[13] J.M.J. Paulusse, R.P. Sijbesma, Ultrasound in polymer chemistry: revival of an established technique, J. Polym. Sci., Polym. Chem. Ed. 44 (19) (2006) 5445–5453, https://doi.org/10.1002/pola.21646.
[14] G.R. Gossweiler, T.B. Kouznetsova, S.L. Craig, Force-rate characterization of two spiropyran-based molecular force probes, J. Am. Chem. Soc. 137 (19) (2015) 6148–6151, https://doi.org/10.1021/jacs.5b02492.
[15] H.M. Klukovich, Z.S. Kean, A.L. Black Ramirez, J.M. Lenhardt, J. Lin, X. Hu, S. L. Craig, Tension trapping of carbonyl ylides facilitated by a change in polymer backbone, J. Am. Chem. Soc. 134 (23) (2012) 9577–9580, https://doi.org/10.1021/ja302996n.
[16] J. Wang, T.B. Kouznetsova, S.L. Craig, Reactivity and mechanism of a mechanically activated anti-Woodward-Hoffmann-DePuy reaction, J. Am. Chem. Soc. 137 (36) (2015) 11554–11557, https://doi.org/10.1021/jacs.5b06168.
[17] J. Wang, T.B. Kouznetsova, Z. Niu, M.T. Ong, H.M. Klukovich, A.L. Rheingold, T. J. Martinez, S.L. Craig, Inducing and quantifying forbidden reactivity with single-molecule polymer mechanochemistry, Nat. Chem. 7 (4) (2015) 323–327, https://doi.org/10.1038/nchem.2185.
[18] A.L. Ramirez, Z.S. Kean, J.A. Orlicki, M. Champhekar, S.M. Elsakr, W.E. Krause, S. L. Craig, Mechanochemical strengthening of a synthetic polymer in response to typically destructive shear forces, Nat. Chem. 5 (9) (2013) 757–761, https://doi.org/10.1038/nchem.1720.
[19] J.M. Lenhardt, A.L.B. Ramirez, B. Lee, T.B. Kouznetsova, S.L. Craig, Mechanistic insights into the sonochemical activation of multimechanophore cyclopropanated polybutadiene polymers, Macromolecules 48 (18) (2015) 6396–6403, https://doi.org/10.1021/acs.macromol.5b01677.
[20] R. Groote, B.M. Szyja, F.A. Leibfarth, C.J. Hawker, N.L. Doltsinis, R.P. Sijbesma, Strain-induced strengthening of the weakest link: the importance of intermediate geometry for the outcome of mechanochemical reactions, Macromolecules 47 (3) (2014) 1187–1192, https://doi.org/10.1021/ma4022339.
[21] S.L. Potisek, D.A. Davis, N.R. Sottos, S.R. White, J.S. Moore, Mechanophore-linked addition polymers, J. Am. Chem. Soc. 129 (45) (2007) 13808–13809, https://doi.org/10.1021/ja076189x.
[22] Z.S. Kean, Z. Niu, G.B. Hewage, A.L. Rheingold, S.L. Craig, Stress-responsive polymers containing cyclobutane core mechanophores: reactivity and mechanistic insights, J. Am. Chem. Soc. 135 (36) (2013) 13598–13604, https://doi.org/10.1021/ja4075997.
[23] Z.S. Kean, A.L. Black Ramirez, Y. Yan, S.L. Craig, Bicyclo[3.2.0]heptane mechanophores for the non-scissile and photochemically reversible generation of reactive bis-enones, J. Am. Chem. Soc. 134 (31) (2012) 12939–12942, https://doi.org/10.1021/ja3063666.
[24] M.J. Kryger, A.M. Munaretto, J.S. Moore, Structure-mechanochemical activity relationships for cyclobutane mechanophores, J. Am. Chem. Soc. 133 (46) (2011) 18992–18998, https://doi.org/10.1021/ja2086728.
[25] H.M. Klukovich, Z.S. Kean, S.T. Iacono, S.L. Craig, Mechanically induced scission and subsequent thermal remending of perfluorocyclobutane polymers, J. Am. Chem. Soc. 133 (44) (2011) 17882–17888, https://doi.org/10.1021/ja2074517.
[26] C.R. Hickenboth, J.S. Moore, S.R. White, N.R. Sottos, J. Baudry, S.R. Wilson, Biasing reaction pathways with mechanical force, Nature 446 (7134) (2007) 423–427, https://doi.org/10.1038/nature05681.
[27] J.M. Clough, R.P. Sijbesma, Dioxetane scission products unchanged by mechanical force, ChemPhysChem 15 (16) (2014) 3565–3571, https://doi.org/10.1002/cphc.201402365.
[28] E. Ducrot, Y. Chen, M. Bulters, R.P. Sijbesma, C. Creton, Toughening elastomers with sacrificial bonds and watching them break, Science 344 (6180) (2014) 186–189, https://doi.org/10.1126/science.1248494.
[29] Y.L. Chen, R.P. Sijbesma, Dioxetanes as mechanoluminescent probes in thermoplastic elastomers, Macromolecules 47 (12) (2014) 3797–3805, https://doi.org/10.1021/ma500598t.
[30] A. Piermattei, S. Karthikeyan, R.P. Sijbesma, Activating catalysts with mechanical force, Nat. Chem. 1 (2) (2009) 133–137, https://doi.org/10.1038/nchem.167.

[31] S. Karthikeyan, S.L. Potisek, A. Piermattei, R.P. Sijbesma, Highly efficient mechanochemical scission of silver-carbene coordination polymers, J. Am. Chem. Soc. 130 (45) (2008) 14968–14969, https://doi.org/10.1021/ja806887k.
[32] F.R. Kersey, W.C. Yount, S.L. Craig, Single-molecule force spectroscopy of bimolecular reactions: system homology in the mechanical activation of ligand substitution reactions, J. Am. Chem. Soc. 128 (12) (2006) 3886–3887, https://doi.org/10.1021/ja058516b.
[33] J. Hawk, S. Craig, Physical and materials applications of pincer complexes, in: G. van Koten, D. Milstein (Eds.), Organometallic Pincer Chemistry, Springer, Berlin Heidelberg, 2013, pp. 319–352.
[34] J.M. Paulusse, J.P. Huijbers, R.P. Sijbesma, Quantification of ultrasound-induced chain scission in PdII-phosphine coordination polymers, Chemistry 12 (18) (2006) 4928–4934, https://doi.org/10.1002/chem.200600120.
[35] J.M.J. Paulusse, J.P.J. Huijbers, R.P. Sijbesma, Reversible, high molecular weight palladium and platinum coordination polymers based on phosphorus ligands, Macromolecules 38 (15) (2005) 6290–6298, https://doi.org/10.1021/ma050561g.
[36] J.M. Paulusse, R.P. Sijbesma, Reversible mechanochemistry of a Pd(II) coordination polymer, Angew. Chem. Int. Ed. Engl. 43 (34) (2004) 4460–4462, https://doi.org/10.1002/anie.200460040.
[37] M.S. Sammon, M. Biewend, P. Michael, S. Schirra, M. Oncak, W.H. Binder, M. K. Beyer, Activation of a copper biscarbene mechano-catalyst using single-molecule force spectroscopy supported by quantum chemical calculations, Chemistry 27 (34) (2021) 8723–8729, https://doi.org/10.1002/chem.202100555.
[38] M. Biewend, S. Neumann, P. Michael, W.H. Binder, Synthesis of polymer-linked copper(I) bis(-heterocyclic carbene) complexes of linear and chain extended architecture, Polym Chem. Uk 10 (9) (2019) 1078–1088, https://doi.org/10.1039/c8py01751d.
[39] P. Michael, S.K.S. Mehr, W.H. Binder, Synthesis and characterization of polymer linked Copper(I) Bis(-heterocyclic carbene) mechanocatalysts, J. Polym. Sci., Polym. Chem. Ed. 55 (23) (2017) 3893–3907, https://doi.org/10.1002/pola.28775.
[40] M. Biewend, P. Michael, W.H. Binder, Detection of stress in polymers: mechanochemical activation of CuAAC click reactions in poly(urethane) networks, Soft Matter 16 (5) (2020) 1137–1141, https://doi.org/10.1039/c9sm02185j.
[41] P. Michael, M. Biewend, W.H. Binder, Mechanochemical activation of fluorogenic CuAAC "click" reactions for stress-sensing applications, Macromol. Rapid Commun. 39 (22) (2018) e1800376, https://doi.org/10.1002/marc.201800376.
[42] S. Funtan, P. Michael, W.H. Binder, Synthesis and mechanochemical activity of peptide-based Cu(I) Bis(N-heterocyclic carbene) complexes, Biomimetics 4 (1) (2019) 24, https://doi.org/10.3390/biomimetics4010024.
[43] K.S. Shinde, P. Michael, W.H. Binder, Mechanochemical activation of a metal–organic framework embedded within a thermoplastic polyurethane matrix: probing fluorogenic stress-sensing, Macromol. Chem. Phys. 224 (23) (2023) 2300297, https://doi.org/10.1002/macp.202300297.
[44] K.S. Shinde, P. Michael, D. Fuhrmann, W.H. Binder, A mechanochemically active metal-organic framework (MOF) based on Cu-Bis-NHC-Linkers: synthesis and mechano-catalytic activation, Macromol. Chem. Phys. 224 (1) (2023) 2200207, https://doi.org/10.1002/macp.202200207.
[45] P. Michael, D. Döhler, W.H. Binder, Improving autonomous self healing via combined chemical/physical principles, Polymer 69 (2015) 216–227, https://doi.org/10.1016/j.polymer.2015.01.041.
[46] D. Döhler, H. Peterlik, W.H. Binder, A dual crosslinked self-healing system: supramolecular and covalent network formation of four-arm star polymers, Polymer 69 (2015) 264–273, https://doi.org/10.1016/j.polymer.2015.01.073.
[47] D. Döhler, P. Zare, W.H. Binder, Hyperbranched polyisobutylenes for self-healing polymers, Polym Chem. Uk 5 (3) (2014) 992–1000, https://doi.org/10.1039/c3py01151h.
[48] M. Schunack, M. Gragert, D. Döhler, P. Michael, W.H. Binder, Low-temperature Cu (I)-Catalyzed "click" reactions for self-healing polymers, Macromol. Chem. Phys. 213 (2) (2012) 205–214, https://doi.org/10.1002/macp.201100377.
[49] D. Döhler, P. Michael, W.H. Binder, Autocatalysis in the room temperature Copper (I)-Catalyzed alkyne–azide “click” cycloaddition of multivalent poly(acrylate)s and poly(isobutylene)s, Macromolecules 45 (8) (2012) 3335–3345, https://doi.org/10.1021/ma300405v.
[50] M. Gragert, M. Schunack, W.H. Binder, Azide/alkyne-"click"-reactions of encapsulated reagents: toward self-healing materials, Macromol. Rapid Commun. 32 (5) (2011) 419–425, https://doi.org/10.1002/marc.201000687.
[51] P. Michael, W.H. Binder, A mechanochemically triggered "click" catalyst, Angew. Chem. Int. Ed. Engl. 54 (47) (2015) 13918–13922, https://doi.org/10.1002/anie.201505678.
[52] K.L. Berkowski, S.L. Potisek, C.R. Hickenboth, J.S. Moore, Ultrasound-induced site-specific cleavage of azo-functionalized poly(ethylene glycol), Macromolecules 38 (22) (2005) 8975–8978, https://doi.org/10.1021/ma051394n.
[53] G. Sivalingam, N. Agarwal, G. Madras, Distributed midpoint chain scission in ultrasonic degradation of polymers, AIChE J. 50 (9) (2004) 2258–2265, https://doi.org/10.1002/aic.10185.
[54] M.W.A. Kuijpers, P.D. Iedema, M.F. Kemmere, J.T.F. Keurentjes, The mechanism of cavitation-induced polymer scission; experimental and computational verification, Polymer 45 (19) (2004) 6461–6467, https://doi.org/10.1016/j.polymer.2004.06.051.
[55] B. Lee, Z. Niu, J. Wang, C. Slebodnick, S.L. Craig, Relative mechanical strengths of weak bonds in sonochemical polymer mechanochemistry, J. Am. Chem. Soc. 137 (33) (2015) 10826–10832, https://doi.org/10.1021/jacs.5b06937.
[56] K.S. Suslick, G.J. Price, Applications of ultrasound to materials chemistry, Annu. Rev. Mater. Sci. 29 (1) (1999) 295–326, https://doi.org/10.1146/annurev.matsci.29.1.295.
[57] G.C. Vougioukalakis, R.H. Grubbs, Ruthenium-based heterocyclic carbene-coordinated olefin metathesis catalysts, Chem. Rev. 110 (3) (2010) 1746–1787, https://doi.org/10.1021/cr9002424.
[58] L.A. Schaper, S.J. Hock, W.A. Herrmann, F.E. Kuhn, Synthesis and application of water-soluble NHC transition-metal complexes, Angew. Chem. Int. Ed. Engl. 52 (1) (2013) 270–289, https://doi.org/10.1002/anie.201205119.
[59] S. Naumann, M.R. Buchmeiser, Latent and delayed action polymerization systems, Macromol. Rapid Commun. 35 (7) (2014) 682–701, https://doi.org/10.1002/marc.201300898.
[60] M.K. Beyer, The mechanical strength of a covalent bond calculated by density functional theory, J. Chem. Phys. 112 (17) (2000) 7307–7312, https://doi.org/10.1063/1.481330.
[61] R. Groote, B.M. Szyja, E.A. Pidko, E.J.M. Hensen, R.P. Sijbesma, Unfolding and mechanochemical scission of supramolecular polymers containing a metal-ligand coordination bond, Macromolecules 44 (23) (2011) 9187–9195, https://doi.org/10.1021/ma201722e.
[62] G.J. Price, The use of ultrasound for the controlled degradation of polymer solutions, Adv. Sonochem. 1 (1990) 231–287.
[63] G.J. Price, P.F. Smith, Ultrasonic degradation of polymer solutions—III. The effect of changing solvent and solution concentration, Eur. Polym. J. 29 (2–3) (1993) 419–424, https://doi.org/10.1016/0014-3057(93)90114-u.
[64] C.E. Diesendruck, J.S. Moore, Mechanophores for self-healing applications, in: W. H. Binder (Ed.), Self-Healing Polymers, Wiley-VCH, Weinheim, 2013, pp. 193–214.
[65] A. Basedow, K. Ebert, Ultrasonic degradation of polymers in solution, Addit. Polym. 22 (1977) 83–148, https://doi.org/10.1007/3-540-07942-4_6.
[66] K.M. Wiggins, J.N. Brantley, C.W. Bielawski, Methods for activating and characterizing mechanically responsive polymers, Chem. Soc. Rev. 42 (17) (2013) 7130–7147, https://doi.org/10.1039/c3cs35493h.
[67] K.S. Suslick, Mechanochemistry and sonochemistry: concluding remarks, Faraday Discuss 170 (0) (2014) 411–422, https://doi.org/10.1039/c4fd00148f.
[68] R. Groote, L. van Haandel, R.P. Sijbesma, The effect of molecular weight and catalyst concentration on catalytic activity in mechanochemically activated transesterification using Silver(I)-Heterocyclic carbene latent catalysts, J. Polym. Sci., Polym. Chem. Ed. 50 (23) (2012) 4929–4935, https://doi.org/10.1002/pola.26323.
[69] M.T. Ong, J. Leiding, H. Tao, A.M. Virshup, T.J. Martinez, First principles dynamics and minimum energy pathways for mechanochemical ring opening of cyclobutene, J. Am. Chem. Soc. 131 (18) (2009) 6377–6379, https://doi.org/10.1021/ja8095834.
[70] J. Ribas-Arino, M. Shiga, D. Marx, Unravelling the mechanism of force-induced ring-opening of benzocyclobutenes, Chemistry 15 (48) (2009) 13331–13335, https://doi.org/10.1002/chem.200902573.
[71] G.I. Bell, Models for the specific adhesion of cells to cells, Science 200 (4342) (1978) 618–627, https://doi.org/10.1126/science.347575.
[72] E. Evans, K. Ritchie, Dynamic strength of molecular adhesion bonds, Biophys. J. 72 (4) (1997) 1541–1555, https://doi.org/10.1016/S0006-3495(97)78802-7.
[73] J. Ribas-Arino, M. Shiga, D. Marx, Understanding covalent mechanochemistry, Angew. Chem. Int. Ed. Engl. 48 (23) (2009) 4190–4193, https://doi.org/10.1002/anie.200900673.
[74] S.S. Konda, J.N. Brantley, C.W. Bielawski, D.E. Makarov, Chemical reactions modulated by mechanical stress: extended Bell theory, J. Chem. Phys. 135 (16) (2011) 164103, https://doi.org/10.1063/1.3656367.
[75] M. Krupicka, D. Marx, Disfavoring mechanochemical reactions by stress-induced steric hindrance, J. Chem. Theor. Comput. 11 (3) (2015) 841–846, https://doi.org/10.1021/ct501058a.
[76] J. Ribas-Arino, D. Marx, Covalent mechanochemistry: theoretical concepts and computational tools with applications to molecular nanomechanics, Chem. Rev. 112 (10) (2012) 5412–5487, https://doi.org/10.1021/cr200399q.
[77] J. VandeVondele, M. Krack, F. Mohamed, M. Parrinello, T. Chassaing, J. Hutter, QUICKSTEP: fast and accurate density functional calculations using a mixed Gaussian and plane waves approach, Comput. Phys. Commun. 167 (2) (2005) 103–128, https://doi.org/10.1016/j.cpc.2004.12.014.
[78] J.P. Perdew, K. Burke, M. Ernzerhof, Generalized gradient approximation made simple, Phys. Rev. Lett. 77 (18) (1996) 3865–3868, https://doi.org/10.1103/PhysRevLett.77.3865.
[79] S. Grimme, J. Antony, S. Ehrlich, H. Krieg, A consistent and accurate ab initio parametrization of density functional dispersion correction (DFT-D) for the 94 elements H-Pu, J. Chem. Phys. 132 (15) (2010) 154104, https://doi.org/10.1063/1.3382344.
[80] J. VandeVondele, J. Hutter, Gaussian basis sets for accurate calculations on molecular systems in gas and condensed phases, J. Chem. Phys. 127 (11) (2007) 114105, https://doi.org/10.1063/1.2770708.
[81] L. Genovese, T. Deutsch, A. Neelov, S. Goedecker, G. Beylkin, Efficient solution of Poisson’s equation with free boundary conditions, J. Chem. Phys. 125 (7) (2006) 074105, https://doi.org/10.1063/1.2335442.